

1 **Using oxygen isotopes to quantitatively assess residual CO₂**
2 **saturation during the CO₂CRC Otway Stage 2B Extension residual**
3 **saturation test**

4 Sascha Serno^{a,*}, Gareth Johnson^a, Tara C. LaForce^{b,c}, Jonathan Ennis-King^{b,c}, Ralf Haese^{b,d},
5 Chris Boreham^{b,e}, Lincoln Paterson^{b,c}, Barry M. Freifeld^{b,f}, Paul J. Cook^{b,f}, Dirk Kirste^{b,g}, R.
6 Stuart Haszeldine^a, Stuart M.V. Gilfillan^a

7

8 ^a School of GeoSciences, The University of Edinburgh, Grant Institute, The King's Buildings, James
9 Hutton Road, Edinburgh EH9 3FE, United Kingdom

10 ^b CO₂CRC Limited, The University of Melbourne, Carlton, VIC 3010, Australia

11 ^c CSIRO Energy, Private Bag 10, Clayton South, Victoria 3169, Australia

12 ^d School of Earth Sciences, The University of Melbourne, Carlton, Victoria 3010, Australia

13 ^e Geoscience Australia, GPO Box 378, Canberra 2601, Australia

14 ^f Lawrence Berkeley National Laboratory, Berkeley, California 94720, United States of America

15 ^g Department of Earth Sciences, Simon Fraser University, 8888 University Drive, Burnaby, British
16 Columbia V5A 1S6, Canada

17

18 *** Corresponding author:** Sascha Serno
19 School of GeoSciences
20 The University of Edinburgh
21 Grant Institute, The King's Buildings
22 James Hutton Road
23 Edinburgh EH9 3FE
24 United Kingdom
25 Phone: +44 1316507010
26 Fax: +44 1316507340
27 Email: Sascha.Serno@ed.ac.uk

28

29 **Abstract**

30 Residual CO₂ trapping is a key mechanism of secure CO₂ storage, an essential
31 component of the Carbon Capture and Storage technology. Estimating the amount of CO₂ that
32 will be residually trapped in a saline aquifer formation remains a significant challenge. Here,
33 we present the first oxygen isotope ratio ($\delta^{18}\text{O}$) measurements from a single-well experiment,
34 the CO₂CRC Otway 2B Extension, used to estimate levels of residual trapping of CO₂.
35 Following the initiation of the drive to residual saturation in the reservoir, reservoir water $\delta^{18}\text{O}$
36 decreased, as predicted from the baseline isotope ratios of water and CO₂, over a time span
37 of only a few days. The isotope shift in the near-wellbore reservoir water is the result of isotope
38 equilibrium exchange between residual CO₂ and water. For the region further away from the
39 well, the isotopic shift in the reservoir water can also be explained by isotopic exchange with
40 mobile CO₂ from ahead of the region driven to residual, or continuous isotopic exchange
41 between water and residual CO₂ during its back-production, complicating the interpretation of
42 the change in reservoir water $\delta^{18}\text{O}$ in terms of residual saturation. A small isotopic distinction
43 of the baseline water and CO₂ $\delta^{18}\text{O}$, together with issues encountered during the field
44 experiment procedure, further prevents the estimation of residual CO₂ saturation levels from
45 oxygen isotope changes without significant uncertainty. The similarity of oxygen isotope-
46 based near-wellbore saturation levels and independent estimates based on pulsed neutron
47 logging indicates the potential of using oxygen isotope as an effective inherent tracer for
48 determining residual saturation on a field scale within a few days.

49

50 **Keywords:** residual saturation, oxygen isotopes, Otway, geochemical tracer, CO₂ storage

51

52

53 1. Introduction

54 Geological storage of CO₂ in rock formations, as part of Carbon Capture and Storage
55 (CCS), is a promising means of directly lowering CO₂ emissions from fossil fuel combustion
56 (Metz et al., 2005). CO₂ can be stored in the subsurface in three different ways over short
57 timescales: (1) structural trapping, where gaseous or liquid CO₂ is trapped beneath an
58 impermeable cap rock, (2) residual trapping, the immobilisation of CO₂ through trapping within
59 individual and dead end spaces between rock grains, and (3) solubility trapping, where CO₂ is
60 dissolved into the reservoir water that fills the pores between rock grains. Mineral trapping of
61 CO₂ as a result of chemical reactions of the injected CO₂ with the host rock, forming new
62 carbonate minerals within the pores, is a longer term storage mechanism, likely to play a role
63 in siliciclastic formations several hundreds of years after initiation of CO₂ injection (e.g.,
64 Audigane et al., 2007; Sterpenich et al., 2009; Xu et al., 2003, 2004; Zhang et al., 2009).

65 For accurately modelling the long term fate of CO₂ in a commercial-scale CCS project,
66 it is of value to develop an efficient plan to quantitatively assess the amount of structural,
67 residual and solubility trapping at the reservoir scale through a short-term test undertaken in
68 the vicinity of an injection well prior to large-scale injection. Such a test would reduce risk and
69 uncertainty in estimating the storage capacity of a formation and would provide a commercial
70 operator with greater reassurance of the viability of their proposed storage site. This is
71 particularly true for residual trapping of CO₂ which can play a major role for CO₂ plume
72 migration, immobilisation, storage security and reservoir management (Doughty and Pruess,
73 2004; Ennis-King and Paterson, 2002; Juanes et al., 2006; Krevor et al., 2015; Qi et al., 2009).
74 Despite the important role of residual trapping of CO₂ in commercial-scale CCS projects, there
75 is a current lack of cost-effective and reliable methodologies to estimate the degree of residual
76 trapping on the reservoir scale (Mayer et al., 2015).

77 Stable isotopes may be highly suitable for assessing the movement and fate of injected
78 CO₂ in the formation since they fingerprint the injected CO₂ rather than being a co-injected

79 compound like perfluorocarbon tracers, Kr or Xe (Mayer et al., 2013). There are few sources
80 of available oxygen other than the reservoir water within CO₂ storage reservoirs (Johnson et
81 al., 2011; Mayer et al., 2015). Any other reservoir oxygen that is available for water-rock
82 reactions is typically in isotopic equilibrium with the reservoir fluid due to relatively fast reaction
83 kinetics in the water-carbonate system (e.g., Mills and Urey, 1940; Vogel et al., 1970). During
84 CO₂ injection, a new major source of oxygen is added to the system in the form of supercritical
85 CO₂. Isotopic equilibrium exchange proceeds rapidly between oxygen in CO₂ and oxygen in
86 water of various salinities (Kharaka et al., 2006; Lécuyer et al., 2009). In most natural
87 environments the amount of oxygen in CO₂ is negligible compared to the amount of oxygen in
88 water. Consequently, the oxygen isotope ratio ($\delta^{18}\text{O}$) of water remains essentially constant
89 and $\delta^{18}\text{O}$ of CO₂ approaches that of the water plus the appropriate isotopic enrichment factor
90 between water and CO₂ ($\epsilon \approx 10^3 \ln \alpha_{\text{CO}_2\text{-H}_2\text{O}}$), depending on the reservoir temperature
91 (Bottinga, 1968). At CO₂ injection sites, due to the large quantities of CO₂ injected, CO₂
92 becomes a major oxygen source, and both CO₂ and water will change their $\delta^{18}\text{O}$ due to
93 isotopic equilibrium exchange reactions if the injected CO₂ is isotopically distinct with respect
94 to the baseline reservoir water (Barth et al., 2015; Johnson and Mayer, 2011; Johnson et al.,
95 2011; Kharaka et al., 2006; Mayer et al., 2015). This has also been observed in natural settings
96 characterised by vast amounts of free-phase CO₂ in contact with water produced from CO₂-
97 rich springs, for example in south east Spain (Céron and Pulido-Bosch, 1999; Céron et al.,
98 1998) or in Bongwana, South Africa (Harris et al., 1997). The change in reservoir water $\delta^{18}\text{O}$
99 due to isotopic exchange with CO₂ under conditions typical for CO₂ injection sites can be
100 related to the fraction of oxygen in the system sourced from CO₂ (Barth et al., 2015; Johnson
101 and Mayer, 2011; Johnson et al., 2011; Kharaka et al., 2006), and the fraction of oxygen
102 sourced from CO₂ can be successfully used to assess volumetric saturation of free-phase and
103 dissolved CO₂ in the reservoir (Johnson et al., 2011; Li and Pang, 2015).

104 CO2CRC Limited (CO2CRC) developed and has operated the CO2CRC Otway Facility
105 in the Otway Basin near Nirranda South, Victoria, Australia, since 2004 (Sharma et al., 2007).

106 The facility allows for trial injection in multiple storage types, including a saline formation that
107 currently uses a single-well configuration. This configuration is ideal for the development of an
108 effective reservoir characterisation test prior to commercial-scale CO₂ injection (Paterson et
109 al., 2011). In 2011, the first single-well injection test (using the CRC-2 injection well) was
110 undertaken at the Otway facility using 150 t of injected CO₂ to quantify reservoir-scale residual
111 trapping of CO₂ in a saline formation in the absence of an apparent structural closure
112 (CO2CRC Otway Stage 2B – henceforth referred to as Otway 2B; Paterson et al., 2011, 2013,
113 2014). The target reservoir for the experiment was within the Paaratte Formation, a saline
114 formation at 1075-1472 m TVDSS (true vertical depth below mean sea level), with the target
115 interval for the Otway 2B experiment at 1392-1399 m TVDSS. Deep saline formations are the
116 most likely candidates for geological CO₂ storage because of their huge potential capacity and
117 their locations close to major CO₂ sources (Holloway, 2001). The Paaratte Formation, while
118 only used for research purposes, is a saline formation analogous to those proposed for
119 commercial-scale CO₂ injection and storage. Two of the original measurements of residual
120 CO₂ saturation were acquired using noble gas (Xe and Kr) tracer injection and recovery data
121 (LaForce et al., 2014), and pulsed neutron logging of the CRC-2 injection well (Schlumberger
122 Residual Saturation Tool; Dance and Paterson, 2016; Paterson et al., 2013, 2014). The
123 second part of the recent CO2CRC Otway Stage 2B Extension project (henceforth referred to
124 as Otway 2B Extension) was a smaller-scale repeat of these two residual saturation tests
125 using improved methodologies.

126 Here we present oxygen ($\delta^{18}\text{O}$) and hydrogen isotope ($\delta^2\text{H}$) data from produced water
127 and formation water (U-tube) samples, and oxygen isotope data from CO₂ samples from the
128 Otway 2B Extension. For the first time we estimate levels of residual trapping of CO₂ based
129 on oxygen isotope data from a single-well test. We compare our results with measures from
130 independent techniques to estimate residual saturation.

131

132

133 **2. CO2CRC Otway Stage 2B Extension Project**

134 The Otway 2B Extension was conducted in October-December 2014 over a time span
135 of 80 days. The target formation for the Otway 2B experiments, the Paaratte Formation, is a
136 complex interbedded formation of medium to high permeability sandstones and thin
137 carbonaceous mud-rich lithologies, deposited in multiple progradations of delta lobes during
138 the Campanian (Bunch et al., 2012; Dance et al., 2012; Paterson et al., 2013). The target
139 interval for the Otway 2B experiments at 1392-1399 m TVDSS is characterised by well-sorted
140 texturally submature deltaic sandstone dominated by quartz and low clay and feldspar
141 contents, overlain by a diagenetic carbonate seal (Kirste et al., 2014; Paterson et al., 2013,
142 2014). The sandstone is characterised by a porosity of ~28%, an average permeability of 2.2
143 Darcy and a fluid salinity of 800 mg/L (Bunch et al., 2012; Dance et al., 2012). The target
144 reservoir is overlain by a cemented interval and a thick non-reservoir lithofacies interval with
145 a high sealing capacity (Paterson et al., 2013, 2014). The CRC-2 well is equipped with a U-
146 tube geochemical sampling system (Freifeld et al., 2005) and a set of four pressure and
147 temperature gauges at the top and bottom of the target interval for the Otway 2B experiments.

148 The aims of the Otway 2B Extension were to study differences in reservoir water quality
149 in response to the injection of CO₂-saturated water with and without trace amounts of gas
150 impurities (Phase 1), and to characterise the residual trapping levels of CO₂ after injection of
151 pure CO₂ into the formation (Phase 2). Our study primarily focuses on Phase 2. However, to
152 study baseline conditions in the reservoir during the entire project, samples were taken during
153 the initial production of 535.8 t of water from the target interval prior to Phase 1 and during the
154 water injection for Phases 1.1 (days 11-12) and 1.2 (days 35-36), the two push-pull tests
155 characterising Phase 1. Further, samples of produced water from Phases 1.1 (day 35) and
156 1.2 (days 62-63) were taken. Operational details of Phase 1 are presented in a separate study
157 (Haese et al., in prep.).

158 Phase 2 started with the production of 75.1 t of water on days 63-64 (Table 1). On day
159 65, 67 t of previously produced water was injected for the 'water test', together with Kr, Xe and
160 methanol dissolved into the water during the injection (Phase 2.1). Water production with U-
161 tube and production water sampling to study the tracer behaviour at reservoir conditions
162 without CO₂ in the formation commenced immediately after the injection, producing 122.2 t of
163 water on days 65-67. A pulsed neutron log was run on day 68 to provide a baseline for the
164 near-wellbore conditions prior to the drive to residual saturation. This was followed by the
165 injection of 109.8 t of pure CO₂ on days 68-72 (Phase 2.2). Immediately following the CO₂
166 injection, another pulsed neutron log was run to measure the CO₂ response to test if the near-
167 well saturation was consistent with the predictions. On days 72-74, 323.7 t of previously
168 extracted water, saturated with 17.5 t of CO₂, was injected to drive the reservoir to residual
169 saturation (Phase 2.3). The injected water that drives the reservoir to residual saturation was
170 fully saturated with CO₂ to avoid dissolving the residually trapped CO₂. The near-well
171 saturation was tested using a final pulsed neutron log. On day 75, 67.2 t of previously produced
172 water, now saturated with 3.9 t of CO₂ and containing trace amounts of Kr, Xe and methanol,
173 was injected, followed by production of 128.5 t of water with U-tube and water sampling over
174 three days. This allowed measurement of the tracer partitioning between water and residually
175 trapped CO₂ in the reservoir during the 'residual saturation test' (Phase 2.4). Finally, the
176 excess water remaining in the surface tanks was re-injected for disposal on days 78-80.
177 Downhole temperatures and pressures were recorded through the entire duration of the
178 project. The injected gas for the Otway 2B Extension was a mix of industrial CO₂ captured at
179 the Callide Oxyfuel pilot capture plant in Queensland (Callide CO₂) and food grade CO₂ (99.9
180 %) from the Boggy Creek well in the vicinity of the Otway site (BOC CO₂).

181

182

183 **3. Materials and Methods**

184 **3.1 Materials**

185 Water and gas samples were collected using the U-tube system (Freifeld et al., 2005).
186 This system provides the advantage of collecting reservoir water at in situ reservoir pressure
187 of ~140 bar, so that the dissolved gas does not exsolve during the ascent of the sample fluid
188 from the reservoir. At Otway, pressurised water samples were collected in 150 mL stainless
189 steel Swagelok cylinders with needle valves on each end. The cylinder was connected to
190 either a 1 L, 5 L or 10 L Restek™ multi-layer gas bag with a polypropylene combo valve,
191 depending on the amount of gas expected. The cylinder was depressurised under controlled
192 conditions for approximately one hour to collect all of the produced CO₂ and other gases in
193 the gas bag. Wet chemical analyses including pH, alkalinity, electrical conductivity and salinity
194 were conducted on the produced water samples in the purpose-built field laboratory. After
195 processing the water samples in the field laboratory, the depressurised fluids were filtered to
196 0.45 µm and ~8 mL of the filtered fluid transferred into a 10 mL pre-evacuated BD® plastic
197 vacutainer through the self-sealing lid of the vacutainer using a hypodermic needle for
198 subsequent isotope analysis.

199 Injection waters were sampled downstream of the oxygen scavenger (see Paterson et
200 al., 2011, for a detailed description and illustration of the CRC-2 process flow setup).
201 Production waters in addition to U-tube samples were sampled directly from the production
202 water line after the degassing tank. The injection and production water samples were filtered
203 to 0.45 µm and transferred to 60 mL Nalgene bottles with tight fitting caps, with zero
204 headspace on filling to prevent evaporation.

205 A sample of the pure CO₂ gas from the nearby Boggy Creek production well (BOC CO₂)
206 was collected for stable isotope analyses in a 1 L gas bag directly from the BOC tanker.
207 Duplicate samples of the Callide industrial CO₂ were collected for isotopic analyses by
208 depressurising a 150 mL stainless steel Swagelok cylinder containing liquid CO₂ filled directly
209 from the Callide tanker.

210

211 **3.2 Methods**

212 Water and CO₂ samples were analysed at the Stable Isotope Geochemistry Laboratory
213 at the School of Earth Sciences of the University of Queensland, Australia. Water samples
214 were analysed for oxygen isotopes after standard CO₂ equilibration (Epstein and Mayeda,
215 1953) and for hydrogen isotopes after online equilibration at 40 °C with Hokko coils, using an
216 Isoprime Dual Inlet Isotope Ratio Mass Spectrometer (DI-IRMS) coupled to a Multiprep Bench
217 for online analysis. Delta values in water samples are reported in ‰ deviation relative to
218 VSMOW (Vienna Standard Mean Ocean Water) for both oxygen and hydrogen isotopes
219 according to

$$220 \quad \delta_{\text{sample}} = \left(\frac{R_{\text{sample}}}{R_{\text{standard}}} - 1 \right) \times 1000 \quad (1)$$

221 where R represents the ¹⁸O/¹⁶O and ²H/¹H ratios of samples and standards, respectively.
222 Analytical uncertainties for water δ²H and δ¹⁸O are ±2 ‰ (1σ – one standard deviation) and
223 ±0.1 ‰ (1σ), respectively. All laboratory standards were calibrated against IAEA (VSMOW,
224 SLAP, GISP) and USGS (USGS45, USGS46) international water standards.

225 CO₂ samples were analysed using an Isoprime/Agilent Gas Chromatograph-
226 combustion-Isotope Ratio Mass Spectrometer (GC-c-IRMS). All samples were analysed using
227 a 20:1 split. The gas chromatograph (GC) (with a 50 m × 320 μm × 5 μm CP-PoraBOND Q
228 column) was set to a flow of 1.2 mL/min with an oven temperature of 40 °C. The δ¹⁸O values
229 of the CO₂ gas (reported in ‰; δ¹⁸O_{CO₂}) were normalised to the VSMOW scale following a 2-
230 point normalisation (Paul et al., 2007). NBS18 and NBS19 international reference standards
231 were analysed to confirm calibration of the δ¹⁸O scale. The analytical uncertainty for δ¹⁸O in
232 gas samples is ±0.2 ‰ (1σ).

233

234

235 **4. Results**

236 **4.1 Hydrogen isotopes in water samples**

237 Values of $\delta^2\text{H}$ in water samples remain relatively constant throughout the entire Otway
238 2B Extension (Fig. 1). All samples bar one of the duplicate samples from the initial water
239 production prior to Phase 1.1 and the first water sample from the CO_2 -saturated water injection
240 of Phase 1.1 fall within the 1σ range ($\pm 1.78 \text{ ‰}$) of the average of all samples from the entire
241 Otway 2B Extension (-30.19 ‰ ; excluding the duplicate sample with much higher values from
242 the initial water production). Four water samples were collected from the injection water during
243 Phase 1.1, and the average of the four ($-33.58 \pm 1.00 \text{ ‰}$) is marginally outside of the 1σ range
244 of the average from all samples. Values of reservoir water $\delta^2\text{H}$ throughout the Otway 2B
245 Extension are similar to baseline reservoir water values during the previous Otway 2B
246 experiment in 2011 (~ -25 to -33 ‰ ; Kirste et al., 2014). The water $\delta^2\text{H}$ of samples collected
247 directly from the production line into bottles and samples from the U-tube during both the water
248 and residual saturation tests show an excellent correlation within their analytical uncertainties.

249

250 **4.2 Oxygen isotopes in water samples**

251 For reservoir water $\delta^{18}\text{O}$, almost all samples prior to the three days of water production
252 for Phase 2.4 fall in the 1σ range (0.19 ‰) of the average of these bottle and U-tube samples
253 (-6.01 ‰) (Fig. 2). This baseline value is similar to the values for the first Otway 2B experiment
254 in 2011 of around -5 to -6 ‰ (Kirste et al., 2014). Only the two samples of injection water for
255 Phase 1.2 ($\delta^{18}\text{O}$ of ~ -5.6 to -5.7 ‰) as well as two samples from the water production prior to
256 Phase 2.1 ($\delta^{18}\text{O}$ of $\sim -6.4 \text{ ‰}$) fall outside of the 1σ range. During the three days of water
257 production for Phase 2.4 (days 75-77), when water samples in contact with CO_2 in the
258 reservoir were collected, a decrease was observed in $\delta^{18}\text{O}$ ratios of reservoir water in both the

259 bottle and U-tube samples to the lowest values recorded throughout the experiment of -6.63
260 ± 0.10 ‰ and -6.46 ± 0.10 ‰, respectively. This indicates a shift away from stable baseline
261 conditions without CO₂ prior to Phase 2.4 (Fig. 2 and 3). In particular, the $\delta^{18}\text{O}$ values of both
262 the bottle and U-tube samples from the last day of water production are clearly lower
263 compared to the baseline conditions, while $\delta^2\text{H}$ values remain constant throughout the entire
264 project (Fig. 3).

265 In contrast to $\delta^2\text{H}$, there is an offset between $\delta^{18}\text{O}$ values in water samples from bottles
266 and the U-tube for the water and residual saturation tests (Fig. 2). Bottle samples have
267 consistently lower $\delta^{18}\text{O}$ values compared to the U-tube samples, although the offset is not
268 constant from sample to sample.

269

270

271 **5. Discussion**

272 **5.1 Baseline Stable Isotope Conditions and Small-Scale Baseline Changes Prior to** 273 **CO₂ Injection**

274 Concurrently increasing or decreasing final water $\delta^{18}\text{O}$ ($\delta^{18}\text{O}_{\text{H}_2\text{O}}^f$) and $\delta^2\text{H}$ values of
275 reservoir water compared to baseline values can indicate admixture of different waters with
276 variable isotopic compositions, while a change in $\delta^{18}\text{O}_{\text{H}_2\text{O}}^f$ without any change in $\delta^2\text{H}$ suggests
277 water-CO₂ interaction in the reservoir when mineral dissolution can be excluded (e.g.,
278 D'Amore and Panichi, 1985; Johnson and Mayer, 2011; Johnson et al., 2011). Both $\delta^{18}\text{O}$ and
279 $\delta^2\text{H}$ of reservoir water prior to CO₂ injection remained relatively stable during these “baseline”
280 conditions, with $\delta^2\text{H}$ of reservoir water showing no change from the stable baseline conditions
281 during the entire Otway 2B Extension (Fig. 1 and 2). This provides strong evidence for no
282 major evaporation or water mixing processes at surface or in the reservoir. Further, both $\delta^{18}\text{O}$

283 and $\delta^2\text{H}$ show similar baseline conditions compared to the 2011 Otway 2B experiment,
284 indicating that any free-phase CO_2 potentially remaining in the reservoir near the well at the
285 end of the previous Otway 2B experiment dissolved and only negligibly changed the $\delta^{18}\text{O}$
286 signature of the reservoir water between the end of the first and initiation of the second Otway
287 2B experiment.

288 This is also supported by numerical simulations that have been run to investigate the
289 distribution of fluids in the reservoir at the start of the Otway Stage 2B Extension. Detailed
290 geological data were used to construct a near-well radial grid for the reservoir unit, and the
291 complete sequence of production and injection of fluids from 2011 onwards, including tracers,
292 was simulated using the TOUGH2 simulator with the EOS7G equation of state module, which
293 can model methane, CO_2 and tracers. The simulations were matched against the relevant field
294 data for pressure, temperature and produced concentrations in the 2011 Otway Stage 2B
295 experiment, so this gives some confidence that the model accurately represents the reservoir
296 behaviour during the 2011 test and beyond. The details of these simulations will be reported
297 elsewhere. By running the model forward from the end of 2011 data, the prediction was that
298 at the beginning of the 2014 experiment, the free-phase CO_2 had been dissolved from the
299 immediate vicinity of the well. Any remaining free-phase CO_2 was predicted to be confined to
300 a thin layer at the top of the reservoir unit, and away from the well.

301 We collected two U-tube samples in duplicate from the initial water production prior to
302 Phase 1.1, and one of these duplicate samples shows higher $\delta^2\text{H}$ values compared to the
303 other U-tube sample collected just prior (Fig. 1). The oxygen isotope composition of the
304 duplicates of both initial water production samples is very similar and within the range of all
305 water samples collected prior to CO_2 injection during Phase 2 (Fig. 2). Since these two
306 samples from the initial water production were stored over six months in a refrigerator in a
307 Falcon tube with around 20 % cap space prior to analysis, and since both samples were
308 collected consecutively and one of the samples shows $\delta^2\text{H}$ values in accordance with the other
309 collected samples during the project (Fig. 1), the higher $\delta^2\text{H}$ values of one of the initial water

310 production samples can potentially be explained by storage contamination influencing only
311 hydrogen isotopes.

312 Only four samples fall outside of the 1σ range of the average of all samples prior to the
313 production phase of the residual saturation test for $\delta^{18}\text{O}$: the two samples of injection water
314 for Phase 1.2 and two samples from the water production prior to the water test. The injection
315 water for Phase 1.2, derived from a different surface storage tank as the water injected during
316 Phase 1.1, shows both slightly higher $\delta^{18}\text{O}$ and $\delta^2\text{H}$ compared to the water injected into the
317 formation around one month earlier during Phase 1.1 (Fig. 1 and 2), potentially indicating
318 minor evaporation processes and/or oxygenation of water in the surface storage tanks (Haese
319 et al., in prep.). At the end of the water production prior to Phase 2.1, more water (212.3 t)
320 was produced than injected during Phases 1.1 and 1.2 (202.2 t). Therefore, it is possible that
321 the last few tons of the water produced was either older reservoir water from prior to the Otway
322 2B Extension or a mixture of this considerably older reservoir water with injected water from
323 Phase 1. This could explain the lower $\delta^{18}\text{O}$ of the waters produced on the day before Phase
324 2.1.

325 The stability of reservoir water $\delta^{18}\text{O}$ prior to Phase 2.4 provides evidence that, with the
326 exceptions noted above, $\delta^{18}\text{O}$ remained stable during baseline conditions when reservoir
327 water was not in contact with free-phase CO_2 . During the three days of water production of
328 Phase 2.4, a decrease in $\delta^{18}\text{O}$ of water in contact with free-phase CO_2 in the reservoir
329 occurred, indicating a clear shift from the stable baseline conditions (Fig. 2 and 3). This change
330 in water $\delta^{18}\text{O}$ can be used in the following to estimate the fraction of CO_2 that is residually
331 trapped in the reservoir.

332

333 **5.2 Estimation of Residual CO_2 Saturation Based on Oxygen Isotope Values of** 334 **Reservoir Water**

335 The method used here to estimate residual CO₂ saturation based on changes in δ¹⁸O of
 336 reservoir water in contact with free-phase CO₂ is described in detail in Johnson et al. (2011).
 337 If the majority of oxygen in the system is sourced from CO₂, as is the case near the injection
 338 well after Phase 2.3, δ¹⁸O<sub>CO₂ will dominate the water-CO₂ system. The δ¹⁸O ratio of reservoir
 339 water will start to change from the baseline water oxygen isotope value, δ¹⁸O_{H₂O}^b, towards an
 340 end-member scenario where the water has a final water value δ¹⁸O_{H₂O}^f lower than that of the
 341 injected CO₂ by the isotopic enrichment factor (Johnson et al., 2011). In this case, the fraction
 342 of oxygen in the system sourced from CO₂, X_{CO₂}^o, can be estimated using</sub>

$$343 \quad X_{CO_2}^o = \frac{(\delta^{18}O_{H_2O}^b - \delta^{18}O_{H_2O}^f)}{(\delta^{18}O_{H_2O}^b + \epsilon - \delta^{18}O_{CO_2})} \quad (2)$$

344 The isotopic enrichment factor ε between CO₂ and water is reported in ‰ and
 345 determined using the equation defined by Bottinga (1968)

$$346 \quad \epsilon = -0.0206 \times \left(\frac{10^6}{T^2}\right) + 17.9942 \times \left(\frac{10^3}{T}\right) - 19.97 \quad (3)$$

347 where T is the reservoir temperature in Kelvin. This equation is valid at atmospheric
 348 conditions as well as elevated temperatures and pressures relevant for CCS projects (Becker
 349 et al., 2015; Bottinga, 1968; Johnson et al., 2011).

350 The water-CO₂ system for oxygen in a reservoir can be described quantitatively in terms
 351 of the averaged reservoir CO₂ saturation for the region contacted by CO₂ and measured with
 352 the water sample (S_{CO₂}) using

$$353 \quad S_{CO_2} = \frac{(BX_{CO_2}^o + CX_{CO_2}^o - B)}{(A - B - AX_{CO_2}^o + BX_{CO_2}^o + CX_{CO_2}^o)} \quad (4)$$

354 with A referring to moles of oxygen in 1 L of free-phase CO₂ at reservoir conditions, B to
 355 moles of oxygen dissolved in 1 L water from CO₂ at reservoir conditions, and C to moles of

356 oxygen in 1 L water at reservoir conditions (Johnson et al., 2011). During Phase 2.3, the
357 injection of CO₂ and water generally matched the target ratio during most of the water injection
358 for the drive to residual. However, late during the injection, there were periods of delivery of
359 added CO₂ below the target, potentially resulting in some dissolution of residually trapped CO₂
360 near the wellbore. Thus, in this experiment estimates of S_{CO₂} based on oxygen isotopes
361 provide flow-weighted averages of CO₂ saturation, and we expect that S_{CO₂} levels in the
362 reservoir are variable over distance from the borehole, with lower saturation estimates near
363 the wellbore.

364 Eq. (4) was first applied during the enhanced oil recovery (EOR) Pembina Cardium CO₂
365 monitoring project in Alberta, Canada, to estimate S_{CO₂} (Johnson et al., 2011), and the
366 robustness of this approach has been validated using laboratory (Barth et al., 2015; Johnson
367 and Mayer, 2011) and theoretical studies (Li and Pang, 2015). It has been further shown by
368 Johnson et al. (2011) that the method outlined above provides S_{CO₂} estimates from the Frio
369 experiment in east Texas (USA) similar to estimates from an approach that did not assume
370 established isotopic equilibrium between water and CO₂ and that uses volumetric ratios of
371 water and CO₂ determined from known changes in water and CO₂ δ¹⁸O (Kharaka et al., 2006).
372 The method can only be applied if isotopic exchange with minerals in the reservoir can be
373 excluded. Injected CO₂ may form carbonic acid and liberate oxygen from the minerals in the
374 reservoir, e.g. through calcite dissolution (Gunter et al., 1993). Based on detailed analyses of
375 all major and minor cations and anions indicating fluid-mineral reactions, including Si, Al, Ca,
376 Mg, K and HCO₃⁻, in reservoir water samples collected during Phase 1 (Haese et al., in prep.),
377 silicate mineral dissolution can be ruled out. Very minor carbonate mineral (calcite and
378 siderite) dissolution was observed. However, the amount of oxygen liberated from carbonate
379 will be very small compared to the total oxygen from CO₂ and water. Sterpenich et al. (2009)
380 demonstrated that less than 1% by mass of an oolitic limestone dissolved due to interaction
381 with CO₂-saturated water under experimental conditions (150 bar, 80 °C) at water-rock ratios
382 40 times higher than those typical for reservoirs considered for CO₂ injection. Further, since

383 the target interval of the reservoir is characterised by deltaic sandstones dominated by quartz
384 and low clay and feldspar contents (Kirste et al., 2014; Paterson et al., 2013, 2014), any
385 contribution of oxygen from dissolution of carbonate minerals to the total oxygen inventory in
386 the target interval is negligible. Therefore, we conclude that we can eliminate isotopic
387 exchange with minerals as a contribution to oxygen isotope changes in the reservoir water
388 during the Otway 2B Extension.

389 As mentioned above, we observe an offset between $\delta^{18}\text{O}$ values in water samples
390 collected directly from the production line and U-tube samples during the water and residual
391 saturation tests, with lower $\delta^{18}\text{O}$ values in bottle compared to U-tube samples, while no change
392 can be observed in $\delta^2\text{H}$ (Fig. 1 and 2). The isotopic equilibrium between water and injected
393 CO_2 is established before CO_2 exsolves (Johnson et al., 2011). Consequently, the U-tube fluid,
394 which is the formation fluid depressurised at atmospheric pressure and therefore not in contact
395 with the atmosphere or reservoir gas over longer time scales, provides our best estimate of
396 $\delta^{18}\text{O}_{\text{H}_2\text{O}}^{\text{f}}$ in the reservoir at the time of sampling. Consequently, we use the U-tube sample
397 values to estimate CO_2 saturation in the following.

398

399 **5.3 Uncertainties in Water and CO_2 Source Mixing**

400 **5.3.1 Water Baselines and Production**

401 For the approach to estimate residual CO_2 saturation outlined above to be robust, it is
402 essential to have a reliable baseline $\delta^{18}\text{O}$ for reservoir water. A total of 390.9 t of CO_2 -saturated
403 water was injected during Phases 2.3 (323.7 t) and 2.4 (67.2 t) prior to producing 128.5 t of
404 water in Phase 2.4 (days 75-77). Consequently, we expect that the water produced in Phase
405 2.4 was a mixture of the injection water of Phases 2.3 and 2.4. The 323.7 t of CO_2 -saturated
406 water injected during Phase 2.3 (days 72-74) had an average water $\delta^{18}\text{O}$ of $-6.07 \pm 0.07 \text{ ‰}$
407 and $\delta^{18}\text{O}_{\text{CO}_2}$ of $+27.65 \pm 0.12 \text{ ‰}$ for the co-injected CO_2 , resulting in a $\delta^{18}\text{O}$ value for the fully

408 CO₂-saturated water of -6.18 ± 0.07 ‰ at wellbore conditions. On day 75, 67.2 t of CO₂-
409 saturated water containing noble gas tracers were injected for Phase 2.4, with an average
410 water $\delta^{18}\text{O}$ of -5.79 ± 0.07 ‰ and $\delta^{18}\text{O}_{\text{CO}_2}$ of $+29.30 \pm 0.20$ ‰ for the co-injected CO₂, resulting
411 in a $\delta^{18}\text{O}$ value for the fully CO₂-saturated water of -5.86 ± 0.07 ‰ at wellbore conditions.

412 The Phase 2.3 (first) injection of CO₂-saturated water thus has a slightly different
413 oxygen isotope signature compared to the injection water for Phase 2.4, resulting in the
414 necessity to account for mixing of these two water masses in the reservoir to provide a reliable
415 baseline value for the estimation of residual saturation on each of the three days of water
416 production. We used the data on co-injected methanol to estimate the mixing ratio of the two
417 water masses during the water production stage. Methanol is a non-reactive tracer that can
418 be applied to study mixing of water masses in a reservoir (e.g., Haese et al., 2013; Tomich et
419 al., 1973). The methanol concentration of the injected water in Phase 2.4 was 330 ± 20 ppm
420 based on duplicate samples from the injection line, and three U-tube samples collected during
421 injection. Methanol was measured in nearly all U-tube samples collected during the water
422 production stage of Phase 2.4. The injected water for Phase 2.3 was sourced from two
423 different water storage tanks, with the last 111 t of the water sourced from the same tank used
424 for the water injection and production during Phase 2.1 (Tank 3), and therefore containing
425 methanol. The other 212 t of the injection were sourced from another tank (Tank 2) containing
426 low levels of methanol (around 25 ppm by mass). Mass balance calculations suggest that the
427 methanol concentration in Tank 3 should have been around 130 ppm at the start of Phase 2.3.
428 Two U-tube samples taken after the Phase 2.3 injection gave an average methanol
429 concentration in the reservoir of 87.5 ppm, suggesting that the injection concentration may
430 have been slightly less than the mass balance calculation would suggest.

431 Fig. 4 shows the U-tube data for the concentration of methanol in the back-produced
432 water in Phase 2.4, with the horizontal axis normalised as the produced volume relative to the
433 injected volume (67.2 t). If there was no mixing between the two masses of injected water,

434 then one would expect this to be a step function, but there is obviously a degree of mixing,
 435 and this is determined by the hydrodynamic dispersion of the reservoir unit around the well.

436 A simple theoretical result can be obtained for the effect of longitudinal dispersion on the
 437 injection of a uniform tracer into a homogeneous reservoir with no initial tracer (Gelhar and
 438 Collins, 1971; Güven et al., 1985), and trivially modified for the case of a uniform background
 439 concentration of tracer already in the reservoir. Let C be the concentration of the tracer in the
 440 produced fluid, C_0 the injected tracer concentration, and C_b the uniform concentration of tracer
 441 already in the reservoir. Let x be the ratio of the cumulative volume of produced fluid at any
 442 time to the volume of the original injected fluid. The ratio of radial dispersivity α to the radial
 443 penetration depth of the tracer, R , is b . If the reservoir is perfectly stratified, and only
 444 longitudinal dispersion is considered, then

$$445 \quad C = (C_0 - C_b) \frac{1}{2} \operatorname{Erfc} \left(\frac{(x-1)}{\left(\frac{16b}{3} \left(2 - |1-x| \frac{1}{2} (1-x) \right) \right)^{1/2}} \right) + C_b \quad (5)$$

446 In our case, it is only the last 111 t of water injected in Phase 2.3 that contain the tracer
 447 concentration C_b . After the injection of 67.2 t in Phase 2.4, the last part of the back-production
 448 of 128.5 t will probably not be producing water beyond that 111 t, so we can consider the
 449 tracer concentration in the reservoir to be uniform. If the theoretical result is fit to the methanol
 450 data by varying C_0 , C_b and b then the curve in Fig. 4 is obtained. The fitted value of C_0 is 331
 451 ppm (with a standard error of 7.2 ppm), which agrees well with the measured concentration of
 452 injected methanol. The fitted value of C_b is 98.6 ppm (with a standard error of 8.7 ppm), which
 453 is close to the measured concentration in the reservoir before the Phase 2.4 injection. The
 454 parameter b has a fitted value of 0.0177 (with a standard error of 0.0055). Numerical
 455 simulations indicate that the average radial penetration depth R of the tracer is about 3.5-3.8
 456 m, so the fitted radial dispersivity α is 0.062 to 0.067 m.

457 The quality of the fit is worst during the early back-production, and this matches with
458 observations made in other similar continuous injection tracer tests (Güven et al., 1985).
459 Hydrodynamic dispersion acts to smooth out tracer concentrations, and since the tracer that
460 was first produced was that last injected (and which has been subject to the least dispersion),
461 this may explain some of the initial scatter in the tracer concentrations.

462 The theory can be extended to take account of permeability contrasts between layers,
463 but for the current test the corresponding result was barely different to the homogeneous case
464 with averaged properties, and so the calculations are not detailed here. Vertical dispersivity
465 has been ignored, although for larger injections into heterogeneous reservoirs this can cause
466 a much longer tail in the back-production, as the tracer disperses from the high permeability
467 layers into the low permeability ones.

468 The fitted analytical theory then gives a straightforward means of estimating the degree
469 of mixing in the reservoir, and the results are summarised in Table 2, where the range of the
470 prediction is obtained by varying the parameter b within the range of the standard error.

471

472 **5.3.2 CO₂ Source**

473 A potential uncertainty in the estimation of residual CO₂ saturation using oxygen
474 isotopes can further result from the mixing of CO₂ from two different sources in the reservoir.
475 The first 12.2 t of the 109.8 t of pure CO₂ injected and residually trapped in the reservoir were
476 Callide CO₂ with a $\delta^{18}\text{O}$ ratio of $+26.05 \pm 0.14$ ‰, while the remaining 97.6 t of pure CO₂ was
477 BOC CO₂ with an oxygen isotope signature of $+29.30 \pm 0.20$ ‰. For the following estimation
478 of residual CO₂ saturation, we assumed perfect mixing of these two CO₂ sources in the
479 reservoir and derived the $\delta^{18}\text{O}_{\text{CO}_2}$ ratio to be used in Eq. (2) as a weighted average based on
480 the amounts of the two injected CO₂ sources. This results in a $\delta^{18}\text{O}_{\text{CO}_2}$ ratio for the residually
481 trapped CO₂ of $+28.94 \pm 0.12$ ‰. We consider this approach as the most reliable to assess

482 $\delta^{18}\text{O}_{\text{CO}_2}$ since we do not have an estimate for the mixing of CO_2 in the reservoir or of variable
483 oxygen isotope signatures of CO_2 in contact with water in the reservoir.

484

485 **5.4 Estimates of Residual CO_2 Saturation in the Paaratte Formation**

486 For each U-tube sample collected for stable isotopes during the three days of water
487 production, we used Eqs. (2)-(4) to estimate residual trapping levels. We used the
488 thermodynamic model of Duan and Sun (2003) to derive solubilities and densities of CO_2 in
489 aqueous NaCl solutions under wellbore conditions for each individual day since temperatures
490 and pressures varied throughout the experiment (Table 3). As mentioned above, the average
491 wellbore temperatures and pressures for the times of U-tube sample collection were derived
492 from the four temperature and pressure gauges in the perforated interval

493 The first water production sample was collected ~7 hours after the start of water
494 production and ~9 hours after the end of CO_2 -saturated water injection. With an isotopic
495 enrichment factor of 36.84 ‰ based on Eq. (3) and a $\delta^{18}\text{O}_{\text{CO}_2}$ value of $+28.94 \pm 0.12$ ‰, we
496 expect the reservoir water in contact with free-phase CO_2 in the reservoir to change to lower
497 $\delta^{18}\text{O}$ values compared to the assumed $\delta^{18}\text{O}_{\text{H}_2\text{O}}^{\text{b}}$ value if isotopic equilibrium exchange
498 between reservoir water and CO_2 is established [Eq. (2)]. Our approach provides a value for
499 $X_{\text{CO}_2}^{\text{o}}$ of 0.13 ± 0.06 (Table 4). This indicates that enough oxygen sourced from CO_2 was
500 available in the reservoir to change the oxygen isotope signature of the reservoir water after
501 only a few hours. The $X_{\text{CO}_2}^{\text{o}}$ value provides a residual saturation estimate based on oxygen
502 isotopes of 14 ± 9 % [Eq. (4)].

503 For the second sample collected on day 76 with a $\delta^{18}\text{O}_{\text{H}_2\text{O}}^{\text{f}}$ value of -6.27 ± 0.10 ‰, the
504 methanol approach indicates that 22 ± 8 % of the oxygen in the water- CO_2 system is sourced
505 from the residually trapped CO_2 , which results in a residual saturation estimate of 28 ± 11 %

506 (Table 4). The sample collected on the last day of Phase 2.4 (day 77) has the lowest $\delta^{18}\text{O}_{\text{H}_2\text{O}}^{\text{f}}$
507 value of all samples collected, with $-6.46 \pm 0.10 \text{ ‰}$, and is clearly distinct from the baseline
508 water $\delta^{18}\text{O}$ prior to the injection of free-phase CO_2 ($-6.01 \pm 0.19 \text{ ‰}$) (Fig. 2 and 3). Our
509 approach provides an $X_{\text{CO}_2}^{\text{o}}$ estimate of $32 \pm 13 \%$ (Table 4). This results in a residual
510 saturation estimate in the target interval of $42 \pm 16 \%$. Our data do not provide information
511 about the timing of established final isotopic equilibrium between oxygen in water and CO_2 in
512 the reservoir, with previous laboratory studies showing that final isotopic equilibrium at
513 reservoir conditions normally encountered during CCS projects (up to 190 bar and $90 \text{ }^\circ\text{C}$) is
514 reached within a one-week period (Becker et al., 2015; Johnson and Mayer, 2011).

515 While our oxygen isotope data from reservoir water show a clear shift as a result of
516 water- CO_2 isotopic exchange in the reservoir within a few days, our estimates of residual CO_2
517 saturation are characterised by relatively large uncertainties. Several factors can result in
518 uncertainties in the oxygen isotope approach. First, and most importantly, the oxygen isotopic
519 distinction between the injected CO_2 and baseline reservoir water in consideration of the
520 isotopic enrichment factor at wellbore conditions is relatively small during the Otway 2B
521 Extension. While a predictable $\delta^{18}\text{O}$ shift to lower values in reservoir water in contact with free-
522 phase CO_2 compared to baseline conditions was observed, the small isotopic distinction of
523 the two main oxygen sources resulted in a small isotopic shift in the short time of the Otway
524 2B Extension and a large uncertainty in S_{CO_2} estimates. Second, there are uncertainties
525 resulting from the field experiment procedure and setup due to variable reservoir conditions
526 during the entire project and uncertainty in the mixing ratios of water masses and CO_2 sources
527 with different isotopic signatures. These uncertainties result in the necessity to make
528 assumptions about mixing ratios of gases and water masses in the reservoir, and about
529 average reservoir conditions during the different phases. The wellbore conditions during the
530 Otway 2B Extension were slightly different compared to the reservoir conditions; in particular,
531 injection temperatures were lower compared to reservoir temperatures ($\sim 59 \text{ }^\circ\text{C}$; Bunch et al.,
532 2012; Dance et al., 2012). Since it is uncertain at which exact temperature the isotopic

533 exchange reactions between free-phase CO₂ and brine occurred in the reservoir, the
534 difference in injection versus reservoir temperature presents an uncertainty in the estimation
535 of residual CO₂ saturation. All these factors can result in larger uncertainties than ideal in the
536 baseline values of CO₂ and reservoir water, and the isotopic enrichment factors assumed for
537 the reservoir.

538

539 **5.5 Comparison of Independent Estimates of Residual CO₂ Saturation**

540 We can compare our residual S_{CO₂} results from the three days of water production to
541 independent estimates of residual CO₂ saturation in the Otway 2B target interval based on
542 noble gas tracers and pulsed neutron logging from the first Otway 2B experiment. For the
543 comparison of results from the two Otway 2B field experiments, we have to consider that
544 differences in residual saturation levels between the two experiments can result from
545 differences in the timing in events, especially during the water flood.

546 All three techniques to be compared measure a spatially varying residual saturation over
547 different depths of investigation using different forms of averaging, and are characterised by
548 specific uncertainties and limitations that have to be considered when comparing the results.
549 Pulsed neutron logging provides residual CO₂ saturation levels in the vicinity of the well (~25
550 cm) at the point of time it is carried out (Adolph et al., 1994; Dance and Paterson, 2016). The
551 CO₂ in the pulsed neutron logging may or may not be residually trapped, using the strict
552 definition of a core test. Pulsed neutron logging and core flooding experiments have further
553 provided evidence that there is a range of residual trapping values throughout a region
554 contacted by CO₂, explained by the Land trapping model (Land, 1968). In this model, the final
555 residual saturation is a function of the maximum CO₂ saturation, and the maximum CO₂
556 saturation varies throughout the region contacted by CO₂ (e.g., Dance and Paterson, 2016;
557 Krevor et al., 2012, 2015; Land, 1968).

558 Tracer tests measure the CO₂ saturation achieved after the drive to residual, and provide
559 a flow-weighted average of residual saturation on a larger reservoir scale compared to pulsed
560 neutron logging, similar to oxygen isotopes. Therefore, the tracer data provide an estimate of
561 residual CO₂ saturation for a larger reservoir rock volume characterised by residually trapped
562 CO₂ and reservoir water (LaForce et al., 2014). The results based on numerical simulations
563 of the noble gas data from the first Otway 2B experiment are potentially prone to uncertainties
564 due to the consideration of a noble gas partitioning coefficients based on noble gas-water
565 experiments at low pressures (Fernández-Prini et al., 2003), while recently new noble gas
566 partitioning coefficients in a supercritical CO₂-water system at reservoir conditions became
567 available and show differences to the previously published ones for low-pressure systems
568 (e.g., Warr et al., 2015).

569 Given the discussed uncertainties and limitations of the techniques, we can now
570 compare the estimates based on oxygen isotope changes in reservoir water with the
571 independent reconstructions of residual CO₂ saturation. The stable isotope sample collected
572 just 7 hours after the start of water production provides a near-wellbore estimate of residual
573 trapping of CO₂, and can therefore be best compared to measures based on pulsed neutron
574 logging. Saturation profiles from the first Otway 2B experiment from pulsed neutron logging
575 show an average residual saturation of 20 %, with an overall range of 7 to 32 % (Dance and
576 Paterson, 2016). While we have to consider the possibility that the water sampled just 7 hours
577 into the water production phase may not have achieved full isotopic equilibrium with residual
578 CO₂ in the reservoir, our estimate for this first stable isotope sample of 14 ± 9 % is similar with
579 the saturation level reconstructed from pulsed neutron logging. The stable isotope sample
580 from the second and third day can be best compared to the estimates based on noble gas
581 injection and recovery. Reconstructed residual CO₂ saturation levels from the multiphase flow
582 simulations of noble gas injection and recovery are between 11 and 20 % for the first Otway
583 2B experiment (LaForce et al., 2014). These estimates fall in the range of possible S_{CO₂} values
584 based on stable isotopes from the second day (28 ± 11 %), but are lower than the results from

585 the last day of the Phase 2.4 water production stage ($42 \pm 16 \%$). This trend of increasing
586 S_{CO_2} with distance from the wellbore based on the oxygen isotope shift in the reservoir water
587 is different to the spatial residual trapping distribution in the reservoir from numerical reservoir
588 simulations, which predict decreasing gas saturation with distance from the well, with residuals
589 not exceeding 20 % further from the injection well.

590 Three potential mechanisms can explain the reconstructed change in oxygen isotopes
591 in the reservoir water during the three days of water production of Phase 2.4. The observed
592 trend can be the result of (1) a higher residual further away from the wellbore that is not
593 reconstructed using the noble gas injection and recovery method, (2) contact of the produced
594 water from the last day of Phase 2.4 with the region of mobile CO_2 ahead of the region driven
595 to residual, and/or (3) higher residual saturation levels reconstructed from oxygen isotopes in
596 waters longer in contact with residually trapped CO_2 in different regions of the reservoir. The
597 region that has been driven to residual does not extend very far into the reservoir and mobile
598 CO_2 from further out may have been pulled towards the well during production. Therefore,
599 mechanism (2) could explain the high S_{CO_2} value reconstructed from the water sampled during
600 the last day of Phase 2.4, but not the higher residual saturation estimate from the second day
601 compared to the first day of water production during Phase 2.4. Mechanism (3) considers
602 alteration of the isotopic values of reservoir water during the back-production that might
603 complicate the interpretation of the oxygen isotope changes in terms of residual saturation in
604 the reservoir. The oxygen isotope shift in the reservoir water away from baseline values may
605 be simply due to the variable CO_2 volumes the waters were in contact with in the reservoir,
606 with water samples characterised by a longer residence time in the supercritical CO_2 -water
607 system from the beginning to end of the production phase. During the back-production of
608 Phase 2.4, the water may have continued exchanging oxygen with residual CO_2 with variable
609 isotopic signatures in the different regions of the reservoir, resulting in further perturbation of
610 $\delta^{18}O_{H_2O}^f$. Since residual CO_2 in the different regions of the reservoir may have already been
611 in contact with other waters and has variable oxygen isotope values compared to the initially

612 injected $\delta^{18}\text{O}_{\text{CO}_2}$ value, and since it is uncertain if there was enough time for continuous
613 isotopic equilibrium exchange of reservoir water on its way to the well during back-production,
614 it is difficult to resolve the potential contribution of mechanism (3) with confidence. Therefore,
615 we cannot estimate the effect of this mechanism for the observed changes in oxygen isotopes
616 of the reservoir water during the experiment.

617 Consequently, we are left with three potential mechanisms to explain the observed
618 oxygen isotope shift in reservoir waters during the residual saturation test, particularly further
619 away from the well. Future modelling and laboratory efforts to study the behaviour of oxygen
620 isotopes in the Paaratte Formation at reservoir conditions, considering timing of injection and
621 production events similar to Stage 2 of the Otway 2B Extension, would help to test our
622 observation of variable residual trapping distribution in the reservoir, and could help further
623 exploring the validity of mechanisms (2) or (3). Until then, all three potential reasons have to
624 be considered in the interpretation of the oxygen isotope shift during the three days of water
625 production, and the true nature of the residual saturation distribution further away from the
626 well remains uncertain. However, mechanisms (2) and (3) are improbable to explain the
627 observed oxygen isotope shift from baseline values for the first stable isotope sample collected
628 shortly after the start of back-production. Therefore, this first water sample is the most reliable
629 of the water production samples in terms of reconstructing residual trapping of CO_2 in the
630 formation. Since the reconstructed residual saturation based on oxygen isotopes from this
631 sample is similar to near-wellbore residual saturation values based on pulsed neutron logging,
632 oxygen isotopes during the Otway 2B Extension show potential as an inherent tracer for
633 residual saturation in a single-well experiment that should be further explored in future field
634 and laboratory experiments.

635

636

637 **6. Conclusions and Future Prospect**

638 Field experiments at EOR sites in Texas (Frio experiment) and Alberta (Pembina
639 Cardium CO₂ monitoring project) provide evidence for the viability of using oxygen isotopes
640 measured in reservoir water and CO₂ to estimate S_{CO_2} over timescales longer than one week
641 (Johnson et al., 2011; Kharaka et al., 2006). This is a parameter that has been difficult to
642 assess using previous monitoring techniques but one which is crucial for determining the
643 efficiency of a CO₂ storage site. The application of oxygen isotopes has further been supported
644 by laboratory rock core experiments (Barth et al., 2015; Johnson and Mayer, 2011), water data
645 from CO₂-rich springs (e.g., Céron and Pulido-Bosch, 1999; Céron et al., 1998; Harris et al.,
646 1997), and theoretical studies (Li and Pang, 2015). Our study is the first to provide evidence
647 for a shift in oxygen isotope ratios of reservoir water due to isotopic equilibrium exchange with
648 free-phase CO₂ in a reservoir over only a few days, compared to stable baseline water values
649 prior to CO₂ injection (Fig. 2 and 3).

650 During Phase 2 of the Otway 2B Extension, the reservoir was characterised by residually
651 trapped CO₂ and fully CO₂-saturated reservoir water. In this setup, oxygen isotope changes in
652 the reservoir water can be used to estimate flow-weighted averages of residual CO₂
653 saturation. Our data provide residual trapping levels for reservoir rock volumes at different
654 distances from the wellbore. The other techniques used to study residual trapping during the
655 first Otway 2B experiment, noble gas tracers and pulsed neutron logging, are variable in their
656 spatial distribution of reconstructed trapping levels and have different depths of investigation
657 in the reservoir. The estimates of residual saturation based on oxygen isotopes from the
658 different days of water production indicate an increase in residual trapping levels with distance
659 from the wellbore. This trend of increasing residual saturation with distance from the wellbore
660 is not consistent with reservoir simulations, which predict the opposite trend. We show that
661 there are three potential mechanisms to explain the observed oxygen isotope shift from
662 baseline values for the water samples further away from the wellbore, resulting in considerable
663 uncertainty about the true residual saturation distribution in the reservoir at distance from the
664 well. However, only isotopic equilibrium exchange between water and residually trapped CO₂

665 can explain the isotopic shift in the water from near the wellbore. The similarity of the oxygen
666 isotope-based result from this water sample with independent estimates based on pulsed
667 neutron logging indicates that monitoring of oxygen isotope ratios of reservoir water in contact
668 with free-phase CO₂ may serve as an inexpensive inherent tracer with potential to reconstruct
669 flow-weighted averages for residual CO₂ saturation on a reservoir scale within a few days
670 without an additional tracer.

671 While our most reliable sample of reservoir water in contact with residually trapped CO₂
672 during the Otway 2B Extension indicates the potential of using oxygen isotopes to reconstruct
673 residual saturation in a single-well experiment, we show that the current setup of the Otway
674 2B Extension is not ideal to reconstruct residual trapping levels further away from the wellbore
675 using this tracer. Further, our residual trapping estimates based on oxygen isotopes are prone
676 to large uncertainties, which is mainly due to the small isotopic distinction of the baseline water
677 and CO₂ values leading to small predictable shifts in δ¹⁸O of reservoir water in contact with
678 the injected CO₂. The setup of the field experiment, with two different sources of CO₂, injection
679 of two CO₂-saturated water masses with different oxygen isotope signatures, and lower
680 injection temperatures compared to reservoir temperatures, results in additional uncertainties
681 in the determination of baseline conditions and in the estimation of S_{CO₂}. For future
682 applications of this inherent tracer in an ideal single-well test, relatively simple measures can
683 be taken to reduce these uncertainties. It should be guaranteed that baseline reservoir water
684 and free-phase CO₂ are isotopically distinct enough to produce large shifts in the reservoir
685 water δ¹⁸O as a result of water-CO₂ oxygen isotope exchange, resulting in small uncertainties
686 in S_{CO₂} estimates. This can be achieved by testing the isotopic signature of both oxygen
687 sources prior to the start of an experiment. In case of a small isotopic distinction, the CO₂ or
688 water to be injected may be isotopically spiked to further the distinction. The injection of CO₂
689 from a single source during the injection of pure CO₂ would increase the reliability and
690 precision of S_{CO₂} estimates. Injection temperatures similar to reservoir conditions further away

691 from the wellbore would further avoid uncertainties in the determination of the oxygen isotopic
692 enrichment factor in the reservoir, but this can be difficult to achieve in field operations.

693

694

695 **Acknowledgements**

696 This work was supported by funding from the UK CCS Research Centre (UKCCSRC)
697 through the Call 2 grant to S.M.V.G., G.J. and R.S.S., and the ECR International Travel
698 Exchange Fund to S.S. The UKCCSRC is funded by the EPSRC as part of the RCUK Energy
699 Programme. Funding for the Otway 2B Extension comes through CO2CRC, AGOS and
700 COSPL. The authors acknowledge the funding provided by the Australian government through
701 its CRC programme to support this CO2CRC research project. Funding for the group from the
702 Lawrence Berkeley National Laboratory was provided by the Carbon Storage Program, U.S.
703 DOE, Assistant Secretary for Fossil Energy, Office of Clean Coal and Carbon Management
704 through the NETL. We would like to thank Sue Golding and Kim Baublys for conducting stable
705 isotope measurements at the Stable Isotope Geochemistry Laboratory of the School of Earth
706 Sciences, University of Queensland, Australia. We appreciate the help in sample collection
707 from Jay Black, Hong Phuc Vu and the field operating team under the supervision of Rajindar
708 Singh. The paper was improved by constructive comments from two anonymous reviewers.

709

710

711 **References**

712 Adolph, B., Brady, J., Flaum, C., Melcher, C., Roscoe, B., Vittachi, A., Schnorr, D., 1994.
713 Saturation monitoring with the RST reservoir saturation tool. *Oilfield Rev.* 6, 29-39.

714 Audigane, P., Gaus, I., Czernichowski-Lauriol, I., Pruess, K., Xu, T.F., 2007. Two-
715 dimensional reactive transport modeling of CO₂ injection in a saline aquifer at the Sleipner
716 site, North Sea. *Am. J. Sci.* 307, 974-1008, doi:10.2475/07.2007.02.

717 Barth, J.A.C., Mader, M., Myrntinen, A., Becker, V., van Geldern, R., Mayer, B., 2015.
718 Advances in stable isotope monitoring of CO₂ under elevated pressures, temperatures and
719 salinities: Selected results from the project CO₂ISO-LABEL, in: Liebscher, A., Münch, U.
720 (Eds.), *Geological Storage of CO₂ - Long Term Security Aspects*. Springer International
721 Publishing, Zürich, Switzerland, pp. 59-71.

722 Becker, V., Myrntinen, A., Nightingale, M., Shevalier, M., Rock, L., Mayer, B., Barth,
723 J.A.C., 2015. Stable carbon and oxygen isotope equilibrium fractionation of supercritical and
724 subcritical CO₂ with DIC and H₂O in saline reservoir fluids. *Int. J. Greenh. Gas Con.* 39, 215-
725 224, doi:10.1016/j.ijggc.2015.05.020.

726 Bottinga, Y., 1968. Calculation of fractionation factors for carbon and oxygen isotopic
727 exchange in system calcite-carbon dioxide-water. *J. Phys. Chem.* 72, 800-808,
728 doi:10.1021/j100849a008.

729 Bunch, M.A., Daniel, R., Lawrence, M., Browne, G., Menacherry, S., Dance, T., Arnot,
730 M., 2012. Multi-scale characterisation of the Paaratte Formation, Otway Basin, for CO₂
731 injection and storage, in: *Proceedings of the AAPG International Conference and Exhibition*
732 2012, Singapore.

733 Céron, J.C., Pulido-Bosch, A., 1999. Geochemistry of thermomineral waters in the
734 overexploited Alto Guadalentín aquifer (South-East Spain). *Wat. Res.* 33, 295-300,
735 doi:10.1016/S0043-1354(98)00175-4.

736 Céron, J.C., Pulido-Bosch, A., de Galdeano, C.S., 1998. Isotopic identification of CO₂
737 from a deep origin in thermomineral waters of southeastern Spain. *Chem. Geol.* 149, 251-258,
738 doi:10.1016/S0009-2541(98)00045-X.

739 D'Amore, F., Panichi, C., 1985. Geochemistry in geothermal-exploration. *Int. J. Energy*
740 *Res.* 9, 277-298, doi:10.1002/er.4440090307.

741 Dance, T., Paterson, L., 2016. Observations of carbon dioxide saturation distribution and
742 residual trapping using core analysis and repeat pulsed-neutron logging at the CO2CRC
743 Otway site. *Int. J. Greenh. Gas Con.* 47, 210-220, doi:10.1016/j.ijggc.2016.01.042.

744 Dance, T., Arnot, M., Bunch, M., Daniel, R., Ennis-King, J., Hortle, A., Lawrence, M.,
745 2012. Geocharacterisation and static modelling of the Lower Paaratte Formation: CO2CRC
746 Otway project stage 2, Technical Report RPT12-3481. CO2CRC, Canberra, Australia.

747 Doughty, C., Pruess, K., 2004. Modeling Supercritical Carbon Dioxide Injection in
748 Heterogeneous Porous Media. *Vadose Zone J.* 3, 837-847, doi:10.2136/vzj2004.0837.

749 Duan, Z.H., Sun, R., 2003. An improved model calculating CO₂ solubility in pure water
750 and aqueous NaCl solutions from 273 to 533 K and from 0 to 2000 bar. *Chem. Geol.* 193, 257-
751 271, doi:10.1016/S0009-2541(02)00263-2.

752 Ennis-King, J., Paterson, L., 2002. Engineering aspects of geological sequestration of
753 carbon dioxide, in: Proceedings of the SPE Asia-Pacific Oil and Gas Conference and
754 Exhibition 2002, Melbourne, Australia.

755 Epstein, S., Mayeda, T., 1953. Variation of O¹⁸ content of waters from natural sources.
756 *Geochim. Cosmochim. Ac.* 4, 213-224, doi:10.1016/0016-7037(53)90051-9.

757 Fernández-Prini, R., Alvarez, J.L., Harvey, A.H., 2003. Henry's constants and vapor
758 liquid distribution constants for gaseous solutes in H₂O and D₂O at high temperatures. *J. Phys.*
759 *Chem. Ref. Data* 32, 903-916, doi:10.1063/1.1564818.

760 Freifeld, B.M., Trautz, R.C., Kharaka, Y.K., Phelps, T.J., Myer, L.R., Hovorka, S.D.,
761 Collins, D.J., 2005. The U-tube: A novel system for acquiring borehole fluid samples from a

762 deep geologic CO₂ sequestration experiment. *J. Geophys. Res.* 110, B10203,
763 doi:10.1029/2005JB003735.

764 Gelhar, L.W., Collins, M.A., 1971. General analysis of longitudinal dispersion in
765 nonuniform flow. *Water Resour. Res.* 7, 1511-1521, doi:10.1029/WR007i006p01511.

766 Gunter, W.D., Perkins, E.H., McCann, T.J., 1993. Aquifer disposal of CO₂-rich gases:
767 Reaction design for added capacity. *Energy Convers. Manage.* 34, 941-948,
768 doi:10.1016/0196-8904(93)90040-H.

769 Güven, O., Falta, R.W., Molz, F.J., Melville, J.G., 1985. Analysis and interpretation of
770 single-well tracer tests in stratified aquifers. *Water Resour. Res.* 21, 676-684,
771 doi:10.1029/WR021i005p00676.

772 Haese, R.R., LaForce, T., Boreham, C., Ennis-King, J., Freifeld, B.M., Paterson, L.,
773 Schacht, U., 2013. Determining residual CO₂ saturation through a dissolution test – Results
774 from the CO₂CRC Otway Project. *Energy Proc.* 37, 5379-5386,
775 doi:10.1016/j.egypro.2013.06.456.

776 Harris, C., Stock, W.D., Lanham, J., 1997. Stable isotope constraints on the origin of
777 CO₂ gas exhalations at Bongwan, Natal. *S. Afr. J. Geol.* 100, 261-266,

778 Holloway, S., 2001 Storage of fossil fuel-derived carbon dioxide beneath the surface of
779 the earth. *Annu. Rev. Energy Env.* 26, 145-166, doi:10.1146/annurev.energy.26.1.145.

780 Hughes, C.E., Crawford, J., 2012. A new precipitation weighted method for determining
781 the meteoric water line for hydrological applications demonstrated using Australian and global
782 GNIP data. *J. Hydrol.* 464-465, 344-351, doi:10.1016/j.hydrol.2012.07.029.

783 Johnson, G., Mayer, B., 2011. Oxygen isotope exchange between H₂O and CO₂ at
784 elevated CO₂ pressures: Implications for monitoring of geological CO₂ storage. *Appl.*
785 *Geochem.* 26, 1184-1191, doi:10.1016/j.apgeochem.2011.04.007.

786 Johnson, G., Mayer, B., Nightingale, M., Shevalier, M., Hutcheon, I., 2011. Using oxygen
787 isotope ratios to quantitatively assess trapping mechanisms during CO₂ injection into
788 geological reservoirs: The Pembina case study. *Chem. Geol.* 283, 185-193,
789 doi:10.1016/j.chemgeo.2011.01.016.

790 Juanes, R., Spiteri, E.J., Orr, F.M., Jr., Blunt, M.J., 2006. Impact of relative permeability
791 hysteresis on geological CO₂ storage. *Water Resour. Res.* 42, W12418,
792 doi:10.1029/2005WR004806.

793 Kharaka, Y.K., Cole, D.R., Hovorka, S.D., Gunter, W.D., Knauss, K.G., Freifeld, B.M.,
794 2006. Gas-water-rock interactions in Frio Formation following CO₂ injection: Implications for
795 the storage of greenhouse gases in sedimentary basins. *Geology* 34, 577-580,
796 doi:10.1130/G22357.1.

797 Kirste, D., Haese, R., Boreham, C., Schacht, U., 2014. Evolution of formation water
798 chemistry and geochemical modelling of the CO₂CRC Otway Site residual gas saturation test.
799 *Energy Proc.* 63, 2894-2902, doi:10.1016/j.egypro.2014.11.312.

800 Krevor, S.C.M., Pini, R., Zuo, L., Benson, S.M., 2012. Relative permeability and trapping
801 of CO₂ and water in sandstone rocks at reservoir conditions. *Water Resour. Res.* 48, W02532,
802 doi:10.1029/2011WR010859.

803 Krevor, S., Blunt, M.J., Benson, S.M., Pentland, C.H., Reynolds, C., Al-Menhali, A., Niu,
804 B., 2015. Capillary trapping for geologic carbon dioxide storage – From pore scale physics to
805 field scale implications. *Int. J. Greenh. Gas Con.* 40, 221-237, doi:10.1016/j.ijggc.2015.04.006.

806 LaForce, T., Freifeld, B.M., Ennis-King, J., Boreham, C., Paterson, L., 2014. Residual
807 CO₂ saturation estimate using noble gas tracers in a single-well field test: The CO₂CRC Otway
808 project. *Int. J. Greenh. Gas Con.* 26, 9-21, doi:10.1016/j.ijggc.2014.04.009.

809 Land, C.S., 1968. Calculation of imbibition relative permeability for two- and three-phase
810 flow from rock properties. *SPE J.* 8, 149-156, doi:10.2118/1942-PA.

811 Lécuyer, C., Gardien, V., Rigaudier, T., Fourel, F., Martineau, F., Cros, A., 2009. Oxygen
812 isotope fractionation and equilibration kinetics between CO₂ and H₂O as a function of salinity
813 of aqueous solutions. *Chem. Geol.* 264, 122-126, doi:10.1016/j.chemgeo.2009.02.017.

814 Li, J., Pang, Z.H., 2015. Environmental isotopes in CO₂ geological sequestration.
815 *Greenh. Gas Sci. Technol.* 5, 1-15, doi:10.1002/ghg.1495.

816 Mayer, B., Shevalier, M., Nightingale, M., Kwon, J.-S., Johnson, G., Raistrick, M.,
817 Hutcheon, I., Perkins, E., 2013. Tracing the movement and the fate of injected CO₂ at the IEA
818 GHG Weyburn-Midale CO₂ Monitoring and Storage Project (Saskatchewan, Canada) using
819 carbon isotope ratios. *Int. J. Greenh. Gas Con.* 16S, S177-S184,
820 doi:10.1016/j.ijggc.2013.01.035.

821 Mayer, B., Humez, P., Becker, V., Dalkhaa, C., Rock, L., Myrntinen, A., Barth, J.A.C.,
822 2015. Assessing the usefulness of the isotopic composition of CO₂ for leakage monitoring at
823 CO₂ storage sites: A review. *Int. J. Greenh. Gas Con.* 37, 46-60,
824 doi:10.1016/j.ijggc.2015.02.021.

825 Metz, B., Davidson, O., de Coninck, H.C., Loos, M., Meyer, L.A., 2005. IPCC Special
826 Report on Carbon Dioxide Capture and Storage. Prepared by Working Group III of the
827 Intergovernmental Panel on Climate Change. Cambridge University Press, Cambridge, UK,
828 442 pp.

829 Mills, G.A., Urey, H.C., 1940. The kinetics of isotopic exchange between carbon dioxide,
830 bicarbonate ion, carbonate ion and water. *J. Am. Chem. Soc.* 62, 1019-1026,
831 doi:10.1021/ja01862a010.

832 Paterson, L., Boreham, C., Bunch, M., Ennis-King, J., Freifeld, B., Haese, R., Jenkins,
833 C., Raab, M., Singh, R., Stalker, L., 2011. The CO₂CRC Otway stage 2B residual saturation
834 and dissolution test: test concept, implementation and data collected – Milestone report to
835 ANLEC 2011, CO₂CRC Publication RPT11-3158. CO₂CRC, Canberra, Australia.

836 Paterson, L., Boreham, C., Bunch, M., Dance, T., Ennis-King, J., Freifeld, B., Haese, R.,
837 Jenkins, C., LaForce, T., Raab, M., Singh, R., Stalker, L., Zhang, Y.Q., 2013. Overview of the
838 CO2CRC Otway residual saturation and dissolution test. *Energy Proc.* 37, 6140-6148,
839 doi:10.1016/j.egypro.2013.06.543.

840 Paterson, L., Boreham, C., Bunch, M., Dance, T., Ennis-King, J., Freifeld, B., Haese, R.,
841 Jenkins, C., Raab, M., Singh, R., Stalker, L., 2014. CO2CRC Otway Stage 2B residual
842 saturation and dissolution test, in: Cook, P.J. (Ed.), *Geologically Storing Carbon: Learning*
843 *from the Otway Project Experience*. CSIRO Publishing, Melbourne, Australia, pp. 343-380.

844 Paul, D., Skrzypek, G., Fórizs, I., 2007. Normalization of measured stable isotopic
845 compositions to isotope reference scales – a review. *Rapid Commun. Mass Spectrom.* 2,
846 3006-3014, doi:10.1002/rcm.3185.

847 Qi, R., LaForce, T.C., Blunt, M.J., 2009. Design of carbon dioxide storage in aquifers.
848 *Int. J. Greenh. Gas Con.* 3, 195-205, doi:10.1016/j.ijggc.2008.08.004.

849 Sharma, S., Cook, P., Berly, T., Anderson, C., 2007. Australia's first geosequestration
850 demonstration project - the CO2CRC Otway Basin Pilot Project. *APPEA J.* 47, 259-270.

851 Sterpenich, J., Sausse, J., Pironon, J., Géhin, A., Hubert, G., Perfetti, E., Grgic, D., 2009.
852 Experimental ageing of oolitic limestones under CO₂ storage conditons: Petrographical and
853 chemical evidence. *Chem. Geol.* 265, 99-112, doi:10.1016/j.chemgeo.2009.04.011.

854 Tomich, J.F., Dalton, R.L., Deans, H.A., Shallenberger, L.K., 1973. Single-well tracer
855 method to measure residual oil saturation. *J. Petrol. Technol.* 25, 211-218, doi:10.2118/3792-
856 PA.

857 Vogel, J.C., Grootes, P.M., Mook, W.G., 1970. Isotopic fractionation between gaseous
858 and dissolved carbon dioxide. *Z. Physik* 230, 225-238, doi:10.1007/BF01394688.

859 Warr, O., Rochelle, C.A., Masters, A., Ballentine, C.J., 2015. Determining noble gas
860 partitioning within a CO₂-H₂O system at elevated temperatures and pressures. *Geochim.*
861 *Cosmochim. Ac.* 159, 112-125, doi:10.1016/j.gca.2015.03.003.

862 Xu, T., Apps, J.A., Pruess, K., 2003. Reactive geochemical transport simulation to study
863 mineral trapping for CO₂ disposal in deep arenaceous formations. *J. Geophys. Res.* 108,
864 2071, doi:10.1029/2002JB001979.

865 Xu, T., Apps, J.A., Pruess, K., 2004. Numerical simulation of CO₂ disposal by mineral
866 trapping in deep aquifers. *Appl. Geochem.* 19, 917-936,
867 doi:10.1016/j.apgeochem.2003.11.003.

868 Zhang, W., Li, Y., Xu, T., Cheng, H., Zheng, Y., Xiong, P., 2009. Long-term variations of
869 CO₂ trapped in different mechanisms in deep saline formations: A case study of the Songliao
870 Basin, China. *Int. J. Greenh. Gas Con.* 3, 161-180, doi:10.1016/j.ijggc.2008.07.007.

871

872

873

874

875

876

877

878

879

880

881 **Figure captions**

882 **Figure 1:** Water $\delta^2\text{H}$ from the Otway 2B Extension. Samples from injection periods
883 (green (CO_2) and blue (water) bars at bottom of graph where numbers indicate tonnage) are
884 shown as open symbols, while samples from production periods (orange bars, number =
885 tonnage) are filled symbols. U-tube samples are shown as triangles, and bottle samples are
886 squares. We differentiate by colour the initial water production and Phase 1.1 (black), Phase
887 1.2 (red), the early production phase in Phase 2 (magenta), Phase 2.1 (blue), and Phases 2.3
888 and 2.4 (green). Error bars show the analytical uncertainty of $\pm 2 \text{ ‰}$. The black line indicates
889 the average of all samples (excluding the duplicate sample with much higher values from the
890 initial water production) $\pm 1\sigma$ uncertainty. Periods of pulsed neutron logging (red bars at
891 bottom) are shown with production data.

892

893 **Figure 2:** Water $\delta^{18}\text{O}$ from the Otway 2B Extension. Samples from injection periods
894 (green (CO_2) and blue (water) bars at bottom of graph where numbers indicate tonnage) are
895 shown as open symbols, while samples from production periods (orange bars, number =
896 tonnage) are filled symbols. U-tube samples are shown as triangles, and bottle samples are
897 squares. We differentiate by colour the initial water production and Phase 1.1 (black), Phase
898 1.2 (red), the early production phase in Phase 2 (magenta), Phase 2.1 (blue), and Phases 2.3
899 and 2.4 (green). Error bars show the analytical uncertainty of $\pm 0.1 \text{ ‰}$. The black line indicates
900 the average of all samples from before the water production of the residual saturation test
901 (prior to day 75) $\pm 1\sigma$ uncertainty. Periods of pulsed neutron logging (red bars at bottom) are
902 shown with production data.

903

904 **Figure 3:** $\delta^{18}\text{O}$ vs. $\delta^2\text{H}$ in water samples from Phases 2.1, 2.3 and 2.4. Samples from
905 injection and production periods are shown as open and filled symbols, respectively. U-tube
906 samples are shown as triangles, and bottle samples as squares. Samples from Phase 2.1 are

907 in blue, from Phase 2.3 in red, from the water injection for Phase 2.4 in magenta, and for the
908 water production of Phase 2.4 in different green colours. The thick black line indicates the
909 local meteoric water line (LMWL) for Melbourne (Hughes and Crawford, 2012), and the black
910 box symbolises the 1σ range of the baseline water samples prior to water production for Phase
911 2.4.

912

913 **Figure 4:** Methanol concentration (ppm) in the back-produced formation water in Phase
914 2.4 (open circles), compared to the fit to a simple analytical theory described in the text (solid
915 line). The horizontal axis is the cumulative produced volume at a given time divided by the
916 total injected volume of 67.2 t.

917

918

919

920

921

922

923

924

925

926

927

928

929 **Tables**

930

931 **Table 1:** Time schedule of Phase 2 of the Otway 2B Extension. Days relate to the start of
 932 the Otway 2B Extension on 3 October 2014.

Day	Phase	Description	Injection CO ₂ (t)	Injection Water (t)	Production Water (t)	Water rate (t/day)	CO ₂ rate (t/day)
63-64		Water production			75.1	50.4	
65	2.1	Water injection with noble gases and methanol		67.0		199.5	
65-67	2.1	Water production			122.2	50.4	
68		Pulsed neutron logging					
68-72	2.2	Pure CO ₂ injection	109.8				32.9
72		Pulsed neutron logging					
72-74	2.3	CO ₂ -saturated water injection	17.5	323.7		155.6	8.4
74		Pulsed neutron logging					
75	2.4	CO ₂ -saturated water injection with noble gases and methanol	3.9	67.2		155.1	9.0
75-77	2.4	Water production			128.5	49.5	

933

934

935

936

937

938

939

940

941 **Table 2:** Results of the methanol analysis for the fraction of the injected CO₂-saturated water
942 mass for Phase 2.4 (second water mass) during the time intervals of U-tube sampling. The
943 results are based on measured methanol concentrations in the U-tube samples and the fitted
944 analytical model.

Day of experiment	Time	Produced water (t)	Fraction of production of second injected CO ₂ -saturated water mass
75	19:45 – 21:15	12.1	1.00
76	17:42 – 19:12	57.4	0.70 ± 0.13
77	19:20 – 20:50	110.2	0.04 ± 0.02

945

946

947

948

949

950

951

952

953

954

955

956

957

958

959 **Table 3:** Wellbore conditions for time periods of U-tube sampling during Phase 2.4. CO₂
 960 solubilities and densities were estimated after Duan and Sun (2003). Parameters A, B and C
 961 are input parameters for Eq. (4).

Day	Time	Average temperature (°C)	Average pressure (bar)	CO ₂ solubility (mol/kg)	CO ₂ density (g/L)	A (mol/L) [Eq. (4)]	B (mol/L) [Eq. (4)]	C (mol/L) [Eq. (4)]
75	19:45 – 21:15	42.47	139.48	1.27	744.01	33.82	2.53	55.51
76	17:42 – 19:12	45.26	139.37	1.24	720.15	32.73	2.48	55.51
77	19:20 – 20:50	47.04	139.34	1.23	704.36	32.02	2.45	55.51

962

963

964

965

966

967

968

969

970

971

972

973

974 **Table 4:** Oxygen isotope-based results of residual CO₂ saturation using Eqs. (2)-(4) for the
 975 three time intervals of U-tube sampling during Phase 2.4.

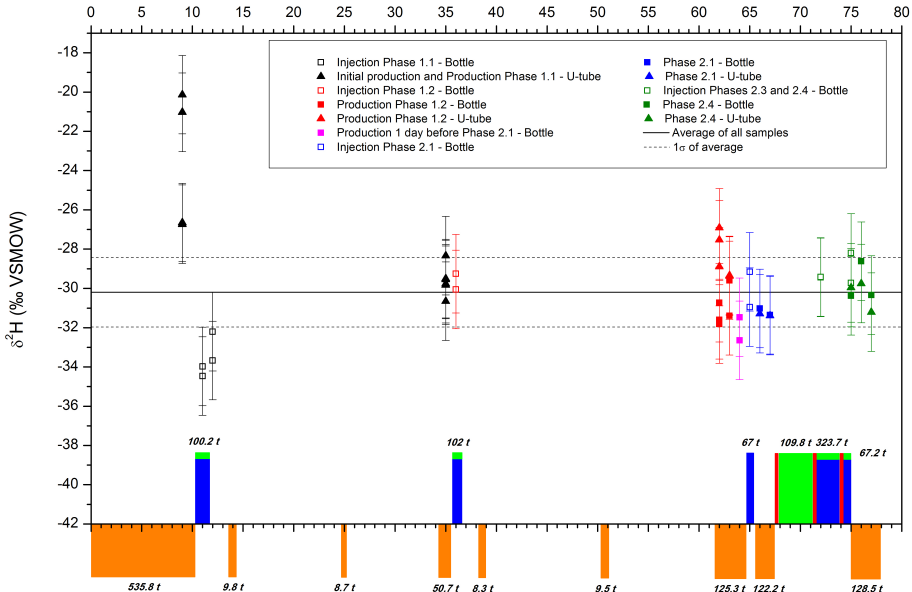
Day of experiment	Time	$\delta^{18}\text{O}_{\text{H}_2\text{O}}^b$ (‰ VSMOW)	ϵ [Eq. (3)] (‰)	$X_{\text{CO}_2}^o$ ¹ [Eq. (2)]	S_{CO_2} [Eq. (4)]
75	19:45 – 21:15	-5.86 ± 0.07	36.84	0.13 ± 0.06	0.14 ± 0.09
76	17:42 – 19:12	-5.96 ± 0.05	36.34	0.22 ± 0.08	0.28 ± 0.11
77	19:20 – 20:50	-6.17 ± 0.07	36.03	0.32 ± 0.13	0.42 ± 0.16

976

977 ¹ Calculated using a constant $\delta^{18}\text{O}_{\text{CO}_2}$ value of +28.94 ± 0.12 ‰ and measured $\delta^{18}\text{O}_{\text{H}_2\text{O}}^f$ values of -6.12 ± 0.10 ‰

978 for day 75, -6.27 ± 0.10 ‰ for day 76, and -6.46 ± 0.10 ‰ for day 77.

Day of CO2CRC Otway Stage 2B Extension



Day of CO2CRC Otway Stage 2B Extension

